Heliyon 10 (2024) e35927

Contents lists available at ScienceDirect

Heliyon

journal homepage: www.cell.com/heliyon

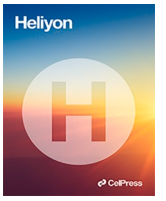

Research article

Oblique pole-side crash assessment using the six-year-old HBM PIPER

Jose L. Torres-Ariza [a,b], Luis Martínez Sáez [b], Christopher R. Torres-San Miguel [a,*]

[a] Instituto Politécnico Nacional, Escuela Superior de Ingeniería Mecánica y Eléctrica, Sección de Estudios de Posgrado e Investigación Unidad Profesional "Adolfo López Mateos", Zacatenco Edificio 5, 2° Piso Col. Lindavista, C.P., 07738, Ciudad de México, Mexico
[b] Universidad Politécnica de Madrid, Instituto Universitario de Investigación del Automóvil Francisco Aparicio Izquierdo (INSIA), Campus Sur UPM, Carretera de Valencia, km 7, 28031, Madrid, Spain

ARTICLE INFO

Keywords:
Biomechanics
Crash
Child
Oblique pole-Side test
PIPER

ABSTRACT

Side impact crashes are one of the most dangerous impact scenarios that a child can suffer. Studies by the National Highway Traffic Safety Administration (NHTSA) have shown that the head and Thorax regions are affected severely. The objective of this work is to perform a numerical evaluation of the oblique pole-side test considering the FMVSS 214-P standard to estimate the Head, Neck, and Thorax injuries for a six-year-old child positioned in the rear seat without any Child Restraint System, two configurations were performed for the oblique pole-side impact: a nearside and a far-side positioning configuration. A six-year-old Human Body Model (HBM) denominated Scalable PIPER Child Model, and the Ford Explorer 2003 were used to perform the test in the LS DYNA® software to assess the biomechanics involved in the crash scenarios. The approach considered a comparative case study with the baseline of the six-year-old child PIPER model to ensure that the positioning adjustment has not affected the mesh quality and interior components for the PIPER child model. The outcomes obtained in case 1 show that the modified PIPER child model has slight outcomes at the shoulder and pelvis zone due to the differences in the body positioning and not by the mesh or the interior interaction between the components. The outcomes obtained in case 2 reflect that the nearside setup obtained the higher measurements for the child occupant. The Ac_{3ms} for Head at nearside test to overcome the Side Criteria established by the Assessment Protocol Child Occupant Protection by Euro NCAP, the kinematics behavior demonstrates the importance of researching children in side crashes to enhance child security, especially in the oblique pole side impact.

1. Introduction

Motor vehicle crashes (MVCs) have been one of the leading health problems over the last decades in the countries. Since passive safety was introduced in the automotive industry, the risk of injury or death decreased. In the beginning, passive safety was focused on enhancing driver and frontal occupant protection (most commonly male adults); later, safety began to be developed to improve child protection in frontal crashes. Despite the efforts that were made, child safety is still lagging due to the lack of studies on children's interaction during side-impact and oblique pole-side collisions. Road traffic injuries are the leading cause of death in children aged

* Corresponding author.
E-mail addresses: jl.torres.ariza@alumnos.upm.es (J.L. Torres-Ariza), luis.martinez@upm.es (L.M. Sáez), ctorress@ipn.mx (C.R. Torres-San Miguel).

https://doi.org/10.1016/j.heliyon.2024.e35927
Received 3 July 2023; Received in revised form 18 June 2024; Accepted 6 August 2024
Available online 12 August 2024

5–14 years in the American region, according to studies by the Pan American Health Organization (PAHO), and one of the leading causes of death for children and young adults aged 5–29 years across several countries [1,2]. As a result, 500 children die on roads globally every 24 h, according to the UN Road Safety Fund (UNRSF) [3] The United Nations International Children's Emergency Fund (UNICEF) shows that injuries in Developed Countries have reported 40 percent of deaths in the age of 1–14 years [4].

According to EURO NCAP, side impact is the second leading cause of death and injuries in Europe [5]. In the case of children, side impact collisions represent one of the most severe injuries and fatalities percentages of occurrences, and the information about injury mechanics is limited [6–8]. Statistical data shows the most common injuries in a side crash included the Head, Chest, and Lower extremities [9]. According to the literature, the Head, the lower and upper extremities, the Thorax, and the abdomen were the main body regions with the most significant injuries for children [10]. Several regulations enhance occupant protection during an oblique pole-side impact, such as the Federal Motor Vehicle Safety Standards (FMVSS) 214 by NHTSA [11], the NCAP protocol [12], the Global Technical Regulation (GTR) No.14 [13], and others. Road Traffic Regulators proposed the protocols to represent a vehicle traveling sideways into a rigid roadside, such as a lamppost or tree [11,12,14]. However, these regulations do not include the use of child dummies to understand their kinematic behavior and the injuries that can be reached in body regions such as the Head, Thorax, and Pelvis.

Numerical oblique pole-side impacts reported in the literature show that the main purpose is to develop alternatives to reduce injuries in adult occupants positioned in the right and left frontal seat [12,15]. On the other hand, some studies were focused on performing an oblique pole-side impact through a sled test to obtain the body injuries with less computational effort and less time [16, 17]. According to the literature, no studies have been reported on child interaction in an oblique pole-side test. The use of child dummies during lateral crash tests is not well defined because the models were developed for frontal crash tests. Child models such as the Hybrid III 6yo and the Q6 have been evaluated in lateral tests, but they have not performed well. On the other hand, HBM models have shown an alternative way to perform different crash tests, such as the PIPER scalable child human body model developed by the EC Funded PIPER project [18], also known as the PIPER child model. The child model has its application in some articles where the main topics were evaluating Child Restraint Systems (CRS) for different child age groups, crash scenarios where the CRS is positioned correctly and with the most common misuses, and accident reconstruction to determine child kinematics behavior [18–31].

This research aims to assess the kinematic behavior and the estimated injury values of a six-year-old child during an oblique pole-side impact. Some crash conditions were applied for the numerical crash test: The FE Explorer 2003 was tested according to the FMVSS 214, and the measurements were compared with the Vehicle Crash Test Databases by NHTSA 4471 [32], 4563 [33], and 4564 [34]. The rear seat was updated with a padding of foam DAX 55, a time interval of 200 ms was defined, and the no use of a CRS was decided following some investigations where constants misuses of a CRS is a highlighted problem, and the no use of a CRS is a real-world problem in many countries [35]. The structure of the paper was defined as follows: in the section Materials and Methods, a comparative analysis of the PIPER child model with the baseline model in two lateral validation tests was performed to compare whether the values from this region are similar or the measurement has some inconsistencies due to the positioning adjustment. Findings from the oblique pole-side impact have shown that the child passenger suffered an important sliding into the seat caused by the absence of a CRS, and the shoulder belt slipped off the thorax region, creating a higher pressure on the neck, and the injuries increased.

2. Materials and methods

The numerical oblique pole-side test performed in this research was proposed to obtain the behavior of a six-year-old child due to any child dummy in the FMVSS 214 being considered. The study is divided into two cases. First, a lateral body evaluation is performed in LS DYNA® to compare the values reported by the baseline PIPER child model with respect to the values obtained by the PIPER child model adjusted to the position of the Explorer's rear seat. The first case is proposed to determine that the child's positioning required does not affect the baseline parts, and the measurements due to a positioning process can affect the mesh quality and create negative volumes and contact problems between the body parts, so an adjustment was carried out with the PIPER software tool (v.1.1.0) The second phase involved a numerical oblique pole-side impact using the child model established in the first case.

The child is restrained using a three-point seatbelt with no retractor and pretensioner, following the Ford Explorer 2003 specification for the seatbelts of the second-row seats. The three-point seatbelt consists of unidimensional (1D) and two-dimensional (2D) with a defined geometric for the belt webbing of 47 mm for the width and a thickness of 1.2 mm. The seatbelt was modeled with the *BELFIT* tool of the LS-Prepost® 4.8 version. In the case of the 1D elements, the card *Section_seatbelt is used, and the constitutive material model by card *B01_Seatbelt was applied with the following properties: a mass per unit length of 8.0×10^{-5} kg/mm to define the stretch characteristics and mass properties for the elements and curves to represent the change of length by the force applied [36]. For the 2D elements, an orthotropic membrane behavior as fabric material is replicated with a membrane shell element formulation, with the parameters ICOMP = 1 and B1–B2 angles of 0 and 90°, respectively. The material applied for the 2D elements was assigned a Fabric constitutive material formulation (Mat_Fabric) with the following properties: a mass density of 1.0×10^{-6} kg/mm^3, a young modulus of 2 GPa in the longitudinal and transverse directions, a Poisson's ratio of 0.3 in both directions and a shear modulus of 0.769 GPa [36].

The 2003 Finite Element model Ford Explorer SUV developed by the Center for Collision Safety and Analysis (CCSA) in conjunction with NHTSA was set up for the numerical oblique pole-side crash test (Fig. 1). The baseline Explorer 2003 model consists of 923 parts, 724628 nodes, and 714205 elements divided into 680288 shell-type elements, 33690 solid elements, and 185 beam elements; the vehicle's total mass is 2024.6 kg [37].

2.1. Child models

Table 1 summarizes the parameters from the HBM PIPER six-year-old child model (Fig. 2). This HBM provides a detailed body child model due to it considers bones, muscles, organs, and anatomical data material in contrast to the Anthropomorphic Test Device (ATD). The model consists of 407 parts describing the anatomical structure and material properties, a total of 139596 nodes, 540058 solid elements, 190527 shell elements, and 751 beam elements. The model mass is 23 kg with a standing height of 1146 mm [18,28,38].

2.2. Dummy positioning process

First, the PIPER six-year-old child model needs to be imported into the PIPER software tool (v.1.1.0) as metadata following the code structure. Table 2 shows the angles applied to the Head, Cervical spine, and lower and upper extremities to reach the position required. The angles were used considering the world reference system for the Head and Cervical Spine rotation. For the other body part, the rotation is relative between the components involved. Following the system reference in Fig. 3, the rotation angles are positive for clockwise rotation and negative angles for anticlockwise.

The *pre-position* module is used to reposition the body parts to a target position. Before the process began, some pre-position parameters were adjusted: the *affine density* was increased to $300/m^{3,}$ and the *target stiffness* was set to 1×10^9. This process was selected to improve the quality of the skin deformation and the stiffness of the joints. The tool *frame-to-frame* was used for the Head and the Cervical Spine. With this tool, a relative frame for every cervical vertebra was established with the angle defined along the y-axis in Table 2, the angles were defined with respect to the world reference. For the rotation is necessary to fix every bone apart from the Cervical Spine and the Head. For the lower and upper extremities, the tool *joint controller* was applied, and the body parts that were not involved in the movement of the body region needed to be fixed. The joint and the angles of rotation were according to the values established in Table 2.

Once the pre-positioning is completed, a postprocessing process is needed for the skin and bone corrections for the rotated body parts. The skin mesh adjustment is made with the *Smooth Surface tool*, and bone corrections are made using the *Kriging module*. The *Smooth Surface* fixes the skin-distorted elements according to the parameters established in Table 3. The corrections for the volume elements with distortions are made with the *Kriging module* with the parameters shown in Table 3. After the process is applied, a Scaled Jacobian metric is computed with the tool *Color by quality* to compute the element quality. Additionally, the *Mesquite Quality Metric* was defined to check 2D and 3D elements, searching for elements with an inverse mean ratio.

2.3. Case study 1

The PIPER child model adjusted to the rear seat Ford Explorer position was subjected to a two-lateral test performed in the Baseline Model by the PIPER project [38]. A shoulder evaluation test according to the test corridors by Irwin et al. [39] and a pelvis evaluation by Ouyang et al. [40] were used to check if the target position defined affects the sensitivity of measurements from the child model.

2.3.1. Boundary conditions of case study 1

The shoulder test for the baseline PIPER child model was performed by Beillas et al. [19,38]. This test established that a rigid impactor of 2.9 kg hits the shoulder with a velocity of 4.5 m/s. The data collected from the evaluation test is the force and the displacement vs time. The upper and lower limits were based on the report by Irwin et al. [39]. Fig. 4a shows the baseline model, and Fig. 4b shows the modified PIPER child model for the shoulder evaluation.

The pelvis evaluation test follows the previous test performed on the baseline model by Beillas et al. [38]. The test evaluates the pelvis response obtained by the interaction with a plate impactor covered with Sorbothane and a fixed opposing plate covered with neoprene foam for a time interval of 30 ms. The pelvis measurement force vs impact displacement was compared with the reported values by Ouyang et al. [40]. Fig. 5b shows the modified child model at the pelvis test evaluation.

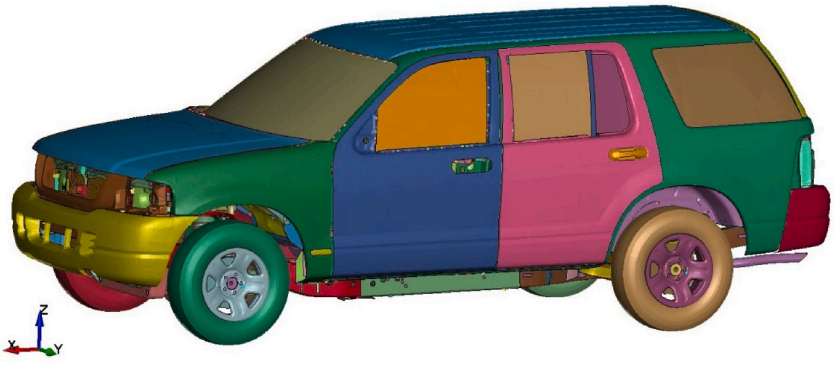

Fig. 1. Baseline Ford Explorer 2003 model.

Table 1
Properties from the FE child models.

	PIPER six-year-old child model
Body parts	407
Nodes	139,596
Solid elements	540,058
Shell elements	190,527
Beam elements	751
Mass (kg)	23

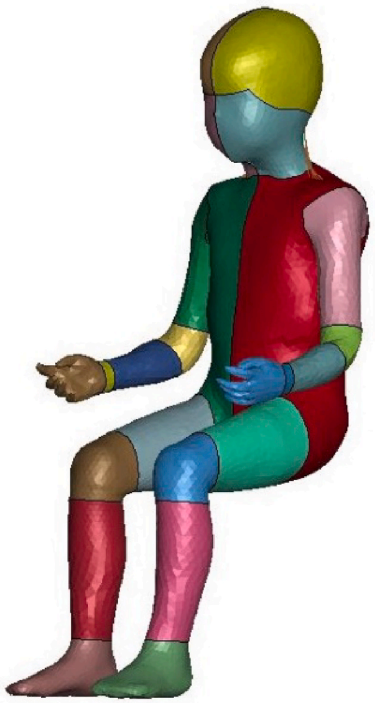

Fig. 2. PIPER six-year-old child model.

Table 2
Angles for the positioning adjustment.

Body region	Reference part	Y-axis	Tool for the rotation
Head	Skull	8°	Frame to frame
Cervical Spine	Atlas, axis Third, fourth, fifth, sixth, and seventh cervical	−10°	Frame to frame
Left upper extremity	Glenohumeral	−12°	Joint controller
	Elbow	20°	Joint controller
	Wrist	0°	Joint controller
Right upper extremity	Glenohumeral	−12°	Joint controller
	Elbow	20°	Joint controller
	Wrist	0°	Joint controller
Left lower extremity	Hip	−12°	Joint controller
	Knee	−50°	Joint controller
	Patella	−20	Joint controller
	Ankle	0°	Joint controller
Right lower extremity	Hip	−12°	Joint controller
	Knee	−50°	Joint controller
	Patella	−20	Joint controller
	Ankle	0°	Joint controller

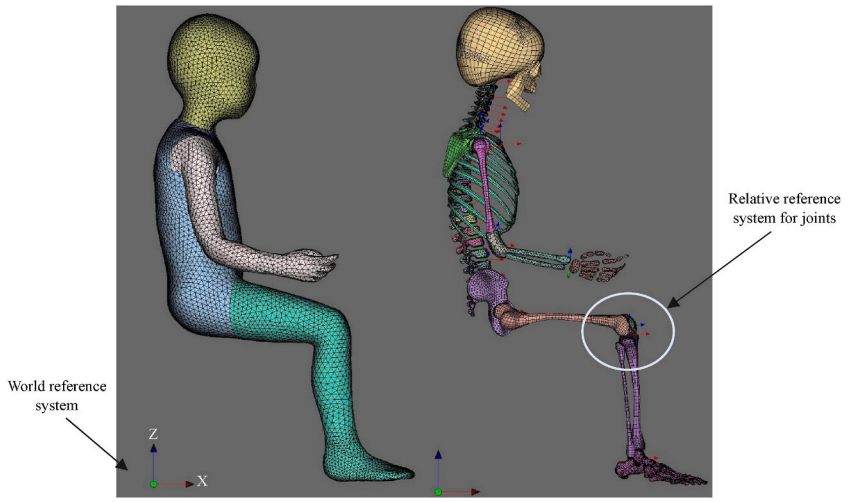

Fig. 3. PIPER child model in the PIPER software framework.

Table 3
Surface and volume smoothing parameters.

Body part	Smooth surface parameters	
	Number of iterations	Passband value
Head skin mesh	50	0.05
Neck skin mesh	50	0.05
Thorax skin mesh	50	0.05
Upper extremity skin mesh	80	0.04
Lower extremity skin mesh	80	0.04
	Kriging module parameters	
Head	50	0.04
Cervical Spine	50	0.04
Upper extremity	50	0.04
Lower extremity	50	0.04

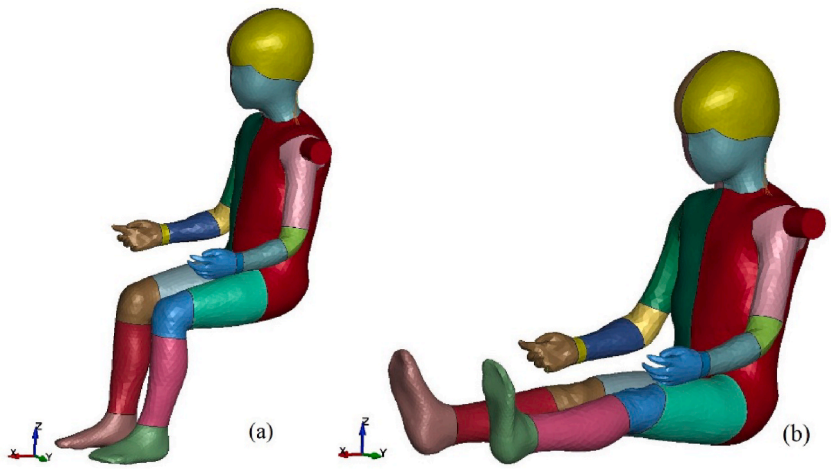

Fig. 4. Shoulder lateral test evaluation a) Baseline PIPER child model b) Modified PIPER child model.

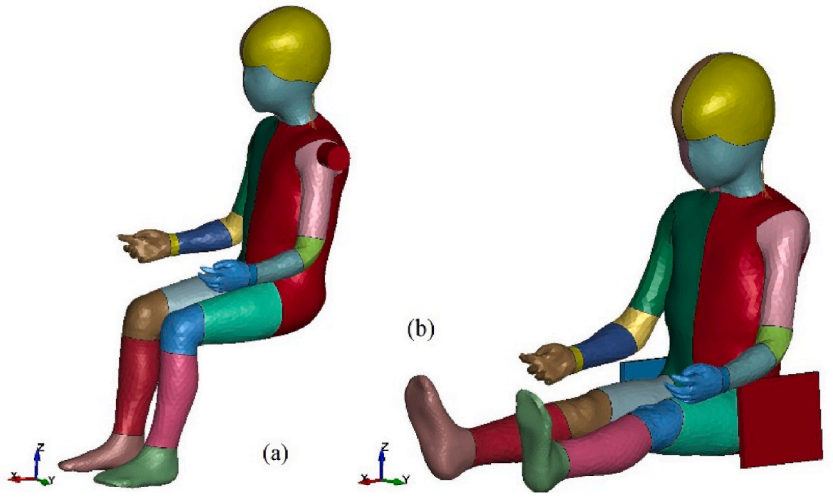

Fig. 5. Pelvis test evaluation a) Baseline model b) Modified PIPER child model.

2.4. Case study 2

An oblique pole side test setup under the FMVSS 214-P by NHTSA was performed to determine the injuries and the kinematic behavior of a six-year-old child during a crash where the vehicle skidded in slippery conditions and hit a pole or a tree.

2.4.1. Boundary conditions of case study 2

The baseline Explorer 2003 model was setup for the numerical oblique pole-side crash test. Table 4 shows a comparative weight distribution between the FE Ford Explorer adjusted for the oblique pole-side test to reach an approximate As Tested Vehicle Weight (ATW) as the Explorer vehicle used in the vehicle crash test databases 4471, 4563, 4564 [32–34].

The time interval defined for the oblique pole-side test is 200 ms, and the test velocity and the impact direction were established according to the test protocol FMVSS 214. The rigid pole was modeled following the geometry and the material properties with a diameter of 254 mm and a rigid material. A Contact_Automatic_Surface_To_Surface between the Ford Explorer and the Rigid pole was defined with a soft constraint formulation SOFT 2 and a segment-based contact type 3 (SBOPT). Fig. 6 show the oblique pole-side test with the child positioned at the lateral impact test (nearside configuration), and Fig. 7 shows the child positioned opposite to the pole impact (far-side configuration).

Additionally, the FE Explorer model was updated in some parts. The front and rear glass from the left windows were deleted to replicate the inside glass into the door from the laboratory test procedure. The rear seat was updated, adding a padding of 30 mm with the foam DAX 55 to the seat structure. The foam was modeled using the constitutive material model *Mat_Low_Density_Foam. The seat cushion and seatback foam were attached to the seat structure with a Constrained_Nodal_Rigid_Body definition, and a Contact_Automatic_Surface_To_Surface was added between the components.

The contacts between the child and the Ford Explorer interior were established with the card

Table 4
Comparative vehicle weights.

	FE Explorer 2003 - Oblique test	Vehicle Crash Test Databases (NHTSA)		
		4471 [32] Report Number: TO11-MGA-2003-001	4563 [33] Report Number: TO11-MGA-2003-006	4564 [34] Report Number: TO11-MGA-2003-004
Unloaded Vehicle Weight (UVW)	2120.69 kg	2138.7 kg	2103.8 kg	2093.3 kg
Dummy Weight/ Configuration	- Additional mass (71.5 kg)/left frontal seat - Child 6yo (23 kg)/Right rear seat	ES-2 (72.4 kg)/Left frontal seat	SID-IIs (44.1 kg)/Left frontal seat	SID-IIs (44.1 kg)/Left frontal seat
Ballast in Cargo Area (kg)	0	0	0	0
Amount of water in Fuel Tank	37.5 lts converted to 37.5 kg distributed additional mass in the fuel tank	0 lts	37.8 lts	30.3 lts
As Tested Vehicle Weight (ATW)	2234.32 kg	2218.6 kg	2218.6 kg	2218.6 kg
Test Velocity	31.7 km/h	31.7 km/h	31.9 km/h	31.7 km/h

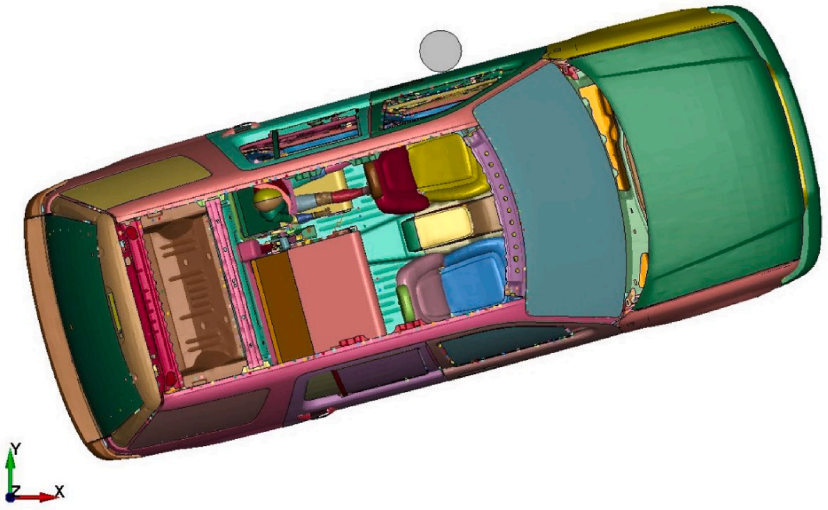

Fig. 6. Test setup for the nearside oblique pole-side impact.

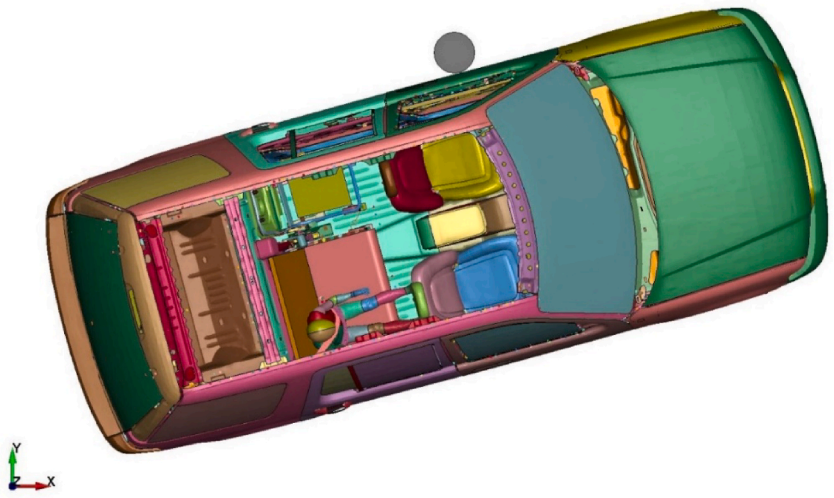

Fig. 7. Test set up for the far-side oblique pole-side impact.

*Contact_Automatic_Surface_To_Surface with a static and dynamic coefficient of friction equal to 0.2, a soft constraint formulation SOFT 2 and a SBOPT 3 with a DEPTH 5. The seatbelt interaction with the child used the same contact definition mentioned with a change in static and dynamic coefficient of friction equal to 0.25.

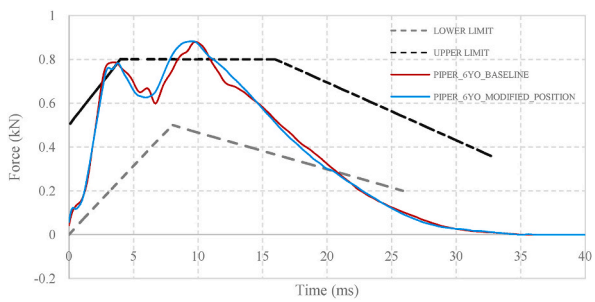

Fig. 8. Force vs time for the shoulder evaluation test.

3. Results

For both case studies the numerical simulations were run using a HPC cluster node with 4 Intel Xeon Platinum 8276L CPUs limited to 80 cores for run the model with LS DYNA R14 MPP single solver.

3.1. Case 1: Lateral evaluation test

For the lateral evaluation test, a 40 ms time interval was performed, and measurements were taken every 1 ms for the shoulder and pelvis region. Figs. 8 and 9 show the comparative response for the force and the deflection obtained for the PIPER six-year-old child model adjusted to the rear seat versus the baseline model. Both models overcome the upper limit value. This behavior was also shown by Beillas et al. [19]. The responses for both models do not show a significant difference in the maximum and minimum values obtained, so the modified child model was not affected by the position and orientation adjustments in the body parts, joints, and contacts from the interior components.

Fig. 10 shows the evaluation for the pelvis zone. According to the values obtained for the modified model, the repositioning process does not affect the response of the baseline model.

3.2. Oblique pole side crash analysis

The data collected from the case studies was filtered using the software DIADEM®. The time interval for the test is 200 ms, with data measurement for Head, Thorax, and Pelvis every 0.1 ms (simulating a sampling rate of 10 kHz). The filters applied for the signal are according to SAE J211 [41]: for the Head and Neck, the filter is CFC 1000, while for the Thorax, a CFC 180 was selected and CFC 600 for pelvis data. Figs. 11 and 12 show the kinematic behavior of the PIPER six-year-old child model during the numerical simulation of the oblique pole-side impact for two rear seat positions: the first position in the Child positioning in the side of the impact (nearside) and opposite (far-side). Both configurations can be divided into four stages of great interest: before the accident with a constant velocity (0 ms), at the vehicle impact into the rigid pole (30 ms), during the interaction between the rigid pole and the vehicle (30–160 ms), and the rebound phase (160–200 ms).

According to the sequence obtained, it is appreciable in the far-side impact that the child lost contact with the seatbelt after 100 ms. One of the main reasons is the seatbelt does not fit properly with the child's body, causing the child to slide along the seat cushion. For the nearside impact, at 80 ms a first contact between the child and the lateral door is observed. The first contact is made with the arms, leg, and Thorax. Subsequently, at 120 ms, the contact between the Head and vehicle door happened, and a severe bounced-back effect was not appreciated due to the Explorer not backing up with a high velocity.

3.2.1. Head measure

The Head Injury Criteria at 15 ms (HIC_{15}) and the Resultant Acceleration at 3 ms (Ac_{3ms}) were proposed to evaluate the data for the Head region. Table 5 shows the head injury criteria for an ATD Q6 child model established in the Assessment protocol Child Occupant Protection by EURO NCAP [42]. The limits show that only the nearside oblique pole-side configurations performed overcome approximately 20 % of the Ac_{3ms} limit, the other head criteria measurements are not within the range sufficient to cause a significant head injury.

The higher head criteria were obtained in the nearside configuration due to the child's head hitting the vehicle door panel. The FE Explorer 2003 does not have door trim, resulting in the steel door material increasing the injury peak value if it is compared with the child's behavior in the far-side configuration where the head interaction was with the seat foam. Fig. 13 shows the HIC_{15} and Ac_{3ms} curves for both crash test configurations as a function of time.

3.2.2. Neck

Neck injuries were obtained considering the resultant force in the upper neck. The measurement in the PIPER child model was considered in the C2–C3. This measure needs to be taken with some limitations due to the Q6 having a different zone of measure. Table 6 shows the resultant force obtained by the oblique test in both configurations. The far-side configuration has a higher resultant

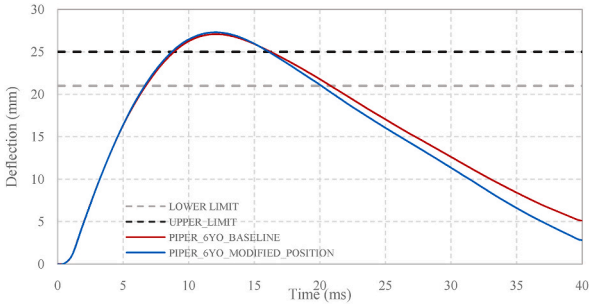

Fig. 9. Deflection vs time for the shoulder evaluation test.

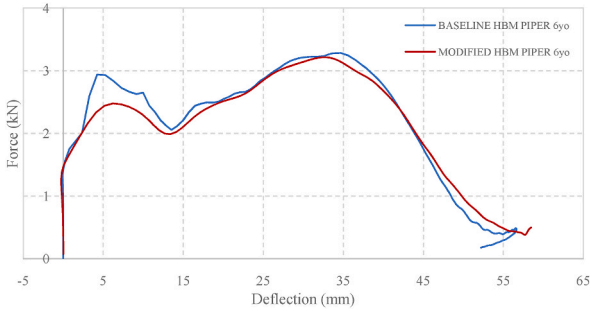

Fig. 10. Force vs deflection for the pelvis test.

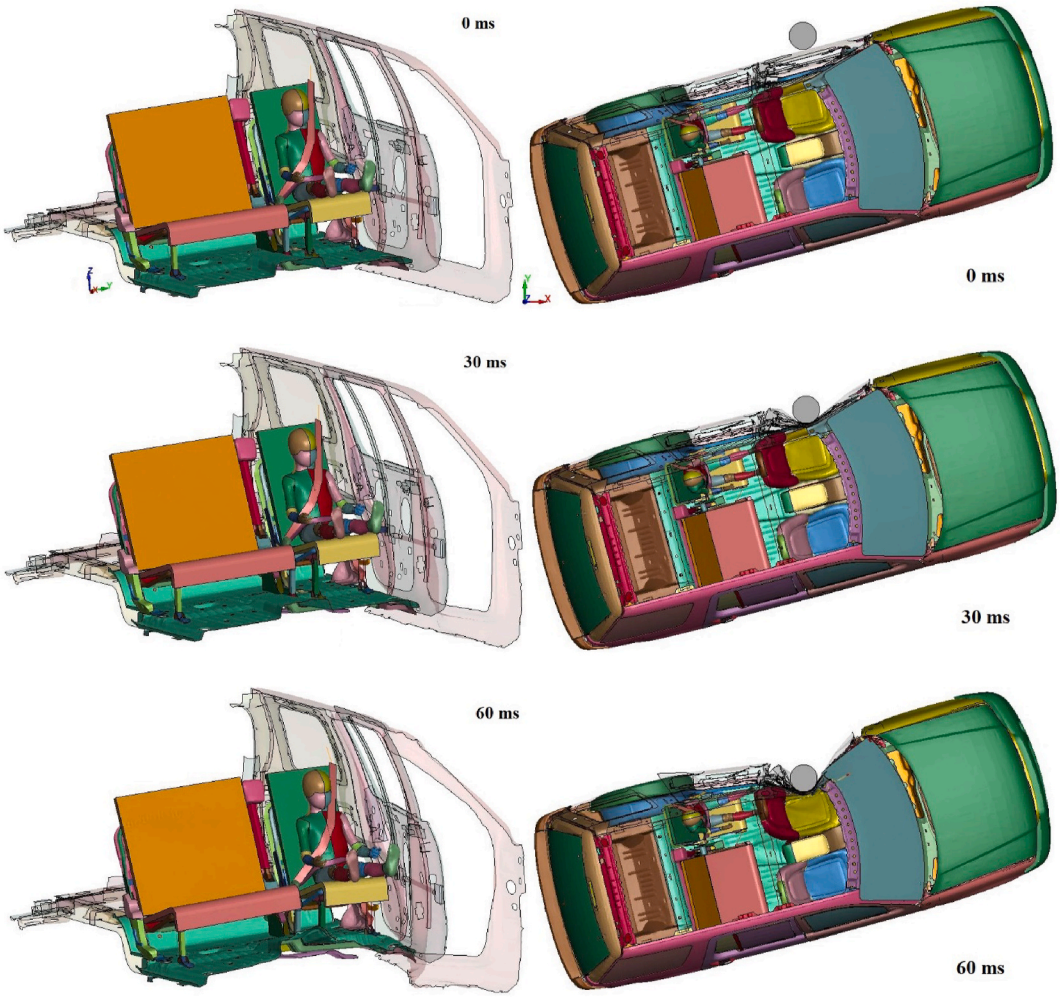

Fig. 11. PIPER six-year-old child kinematics in oblique pole-side impact at nearside impact.

force since the child has a slide movement along the seat due to the child losing contact with the seatbelt due to the absence of a CRS, and neck rotation was observed according to the child kinematics shown in Fig. 12 for the far-side test. Fig. 14 illustrates the upper neck measurements at the three axes and the resultant force as a function of time. Fig. 15 reports the criteria evaluation reached by the PIPER six-year-old Child model during both oblique pole-side setups with the EURO NCAP values (see Table 7).

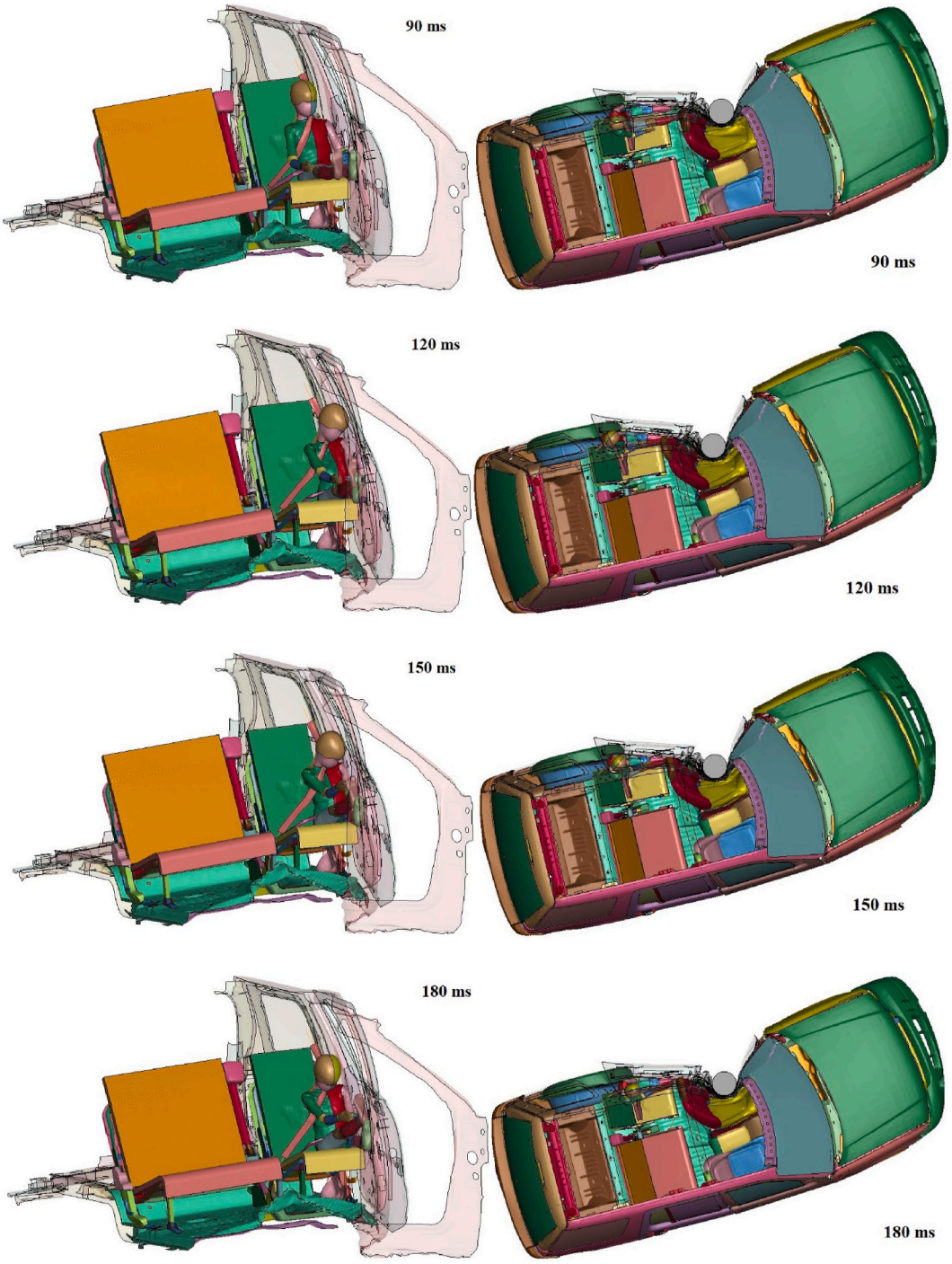

Fig. 11. (*continued*).

3.2.3. Thoracic spine

The thoracic spine's Resulting acceleration at 3 ms was filtered with CFC 180. Based on the kinematics response, the maximum peak acceleration for the nearside configuration occurs at 105.35 ms when the child hits the lateral door for the first time. The far-side maximum peak acceleration is reached at 105.25 ms when the seatbelt reaches the maximum displacement, and a high force of restraint is applied to the child's pelvis region. Fig. 16 shows the curves from the thoracic acceleration at 3 ms for both configurations.

The pelvis acceleration in the three axes is reported as a complementary measurement due to the pelvis region having two interactions of great interest: the lap belt contact with the pelvis during the far-side configuration and the hit with the lateral door during

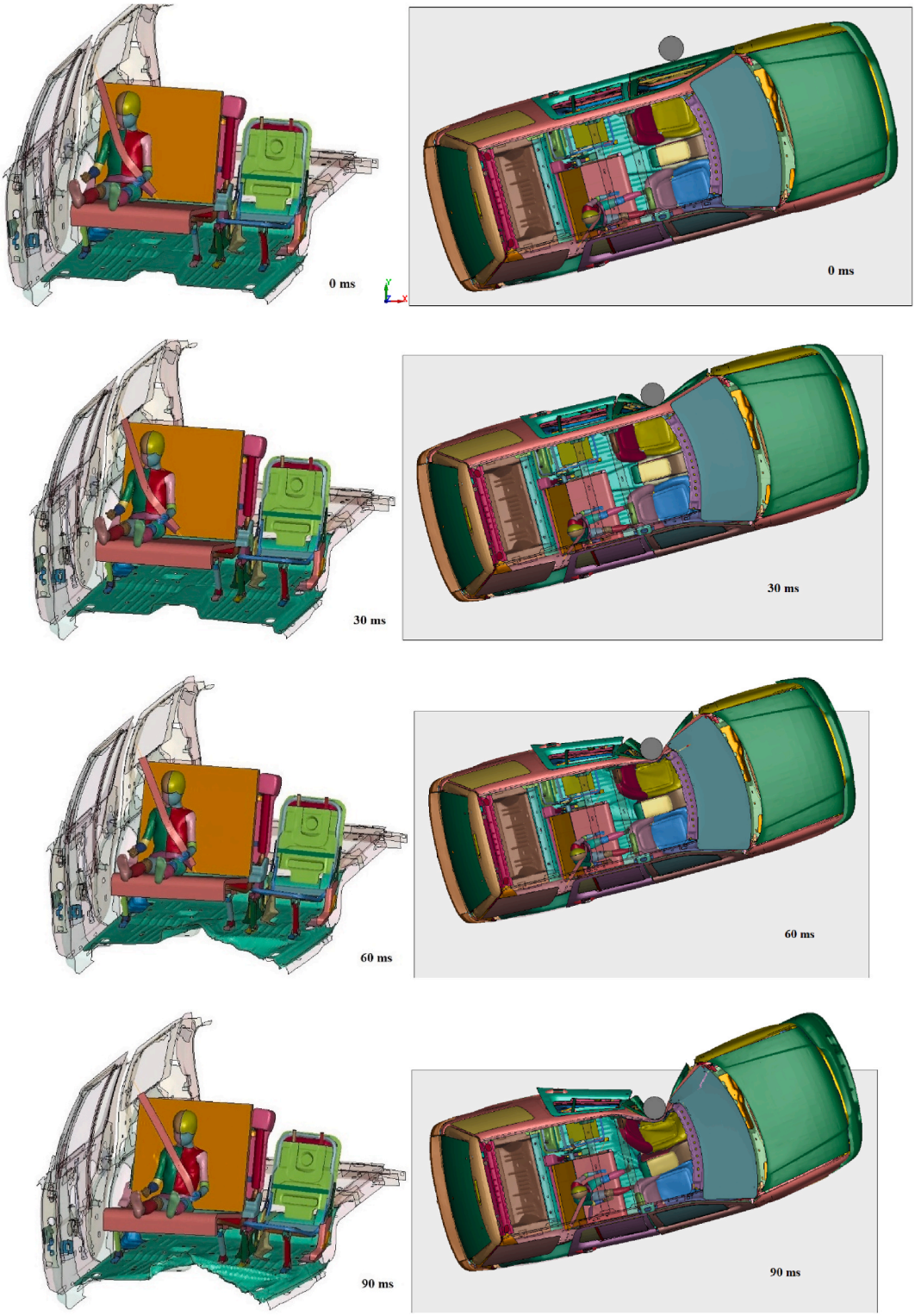

Fig. 12. PIPER six-year-old child kinematics in oblique pole-side impact at far-side impact.

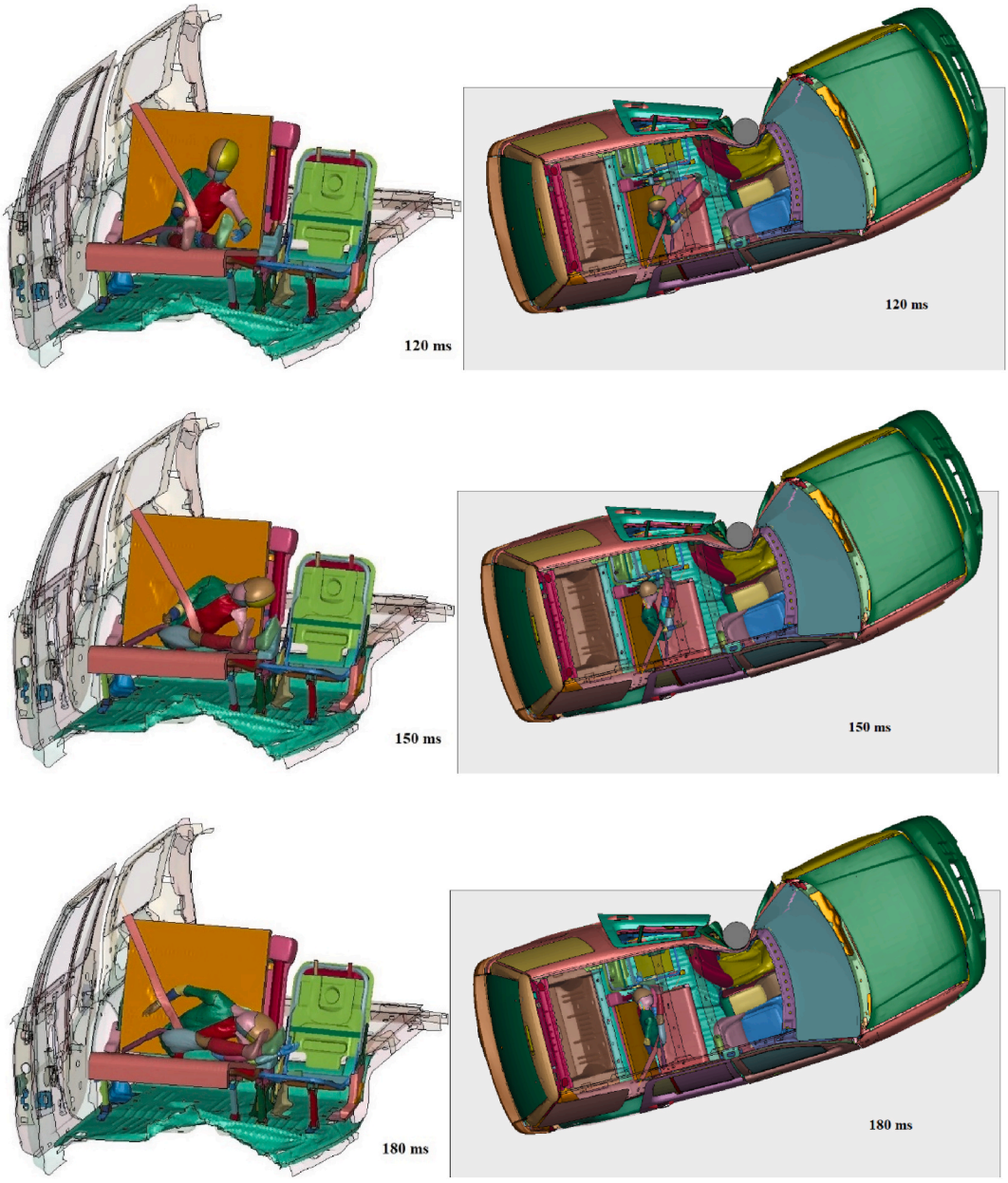

Fig. 12. (*continued*).

Table 5
Head criteria obtained for the oblique pole side test.

Head Criteria	Oblique pole-side far-side configuration	Oblique pole-side nearside configuration	EURO NCAP [42]		
			Higher Limit	Lower Limit	Capping
HIC_{15}	164.5	506.7	500	700	800
Ac_{3ms}	41.6 g	96.8 g	60 g	80 g	80 g
Ac max	153.45 g	113.49 g	–	–	–

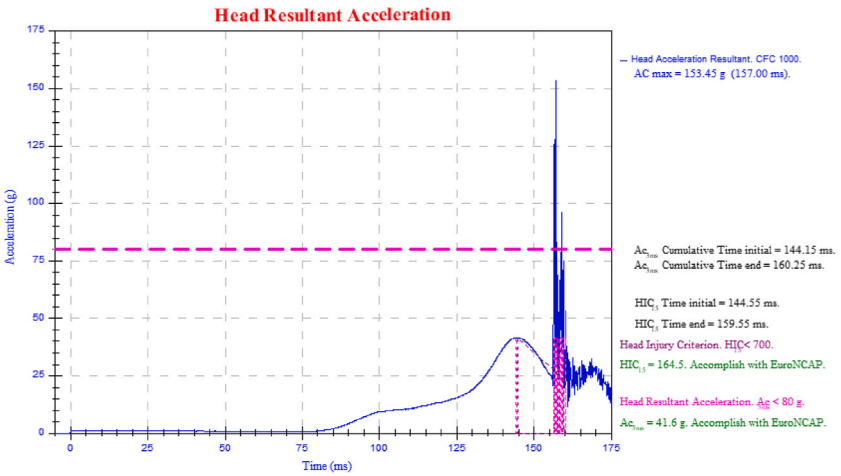

(a)

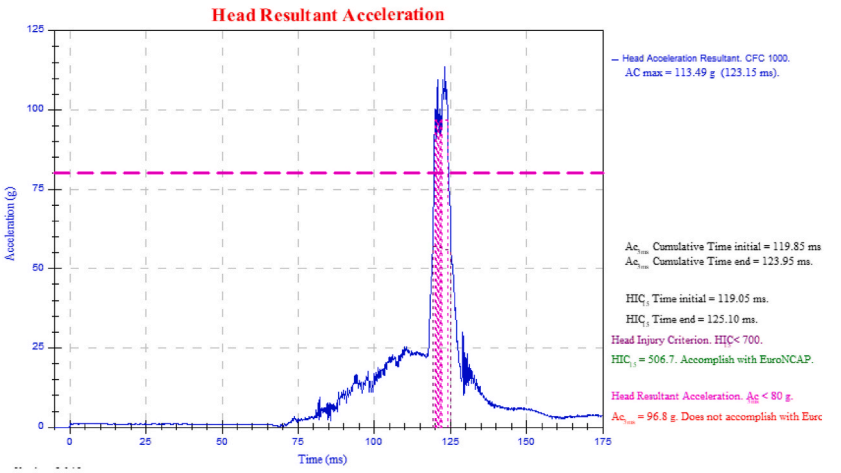

(b)

Fig. 13. HIC_{15} and Ac_{3ms} for the PIPER six-year-old child (a) far-side (b) nearside.

Table 6
Neck criteria obtained for the oblique pole side test.

Neck Criteria	Oblique pole-side far-side configuration	Oblique pole-side nearside configuration	EURO NCAP [42]		
			Higher Limit	Lower Limit	Capping
Resultant force	0.775 kN	0.585 kN	–	2.4 kN	–

Table 7
Thorax criteria obtained for the oblique pole side test.

Thorax Criteria	Oblique pole-side far-side configuration	Oblique pole-side nearside configuration	EURO NCAP [42]		
			Higher Limit	Lower Limit	Capping
Resultant 3 ms acceleration	22	45	–	67 g	–

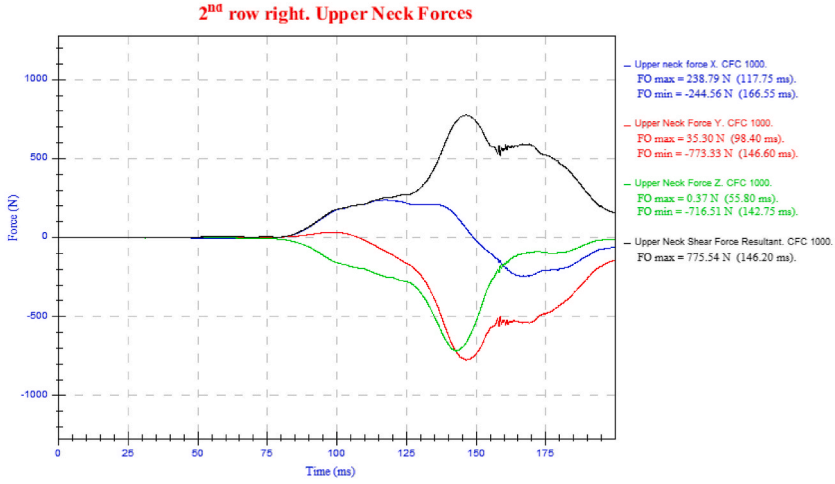

(a)

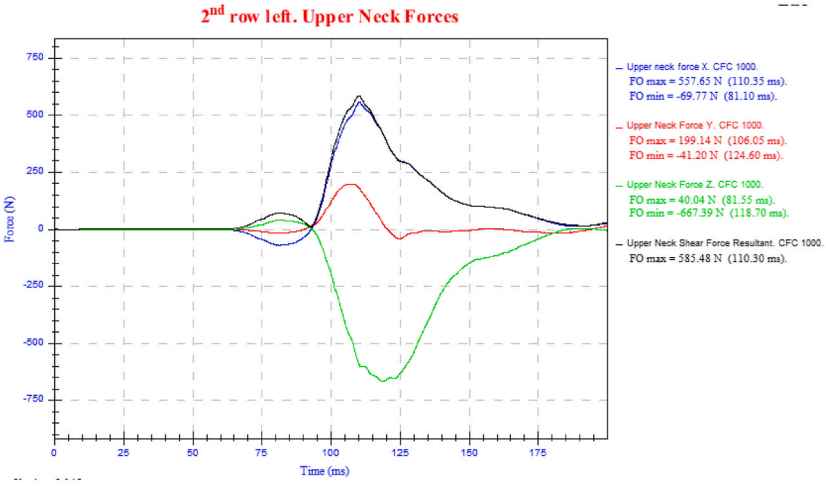

(b)

Fig. 14. Upper neck forces by the PIPER six-year-old child (a) far-side (b) nearside.

the nearside configuration. The pelvis was not compared with any injury criteria due to any value found by Road Traffic Regulators for a child in a side impact. Fig. 17 shows the curves for both configurations filtered with CFC 600.

4. Discussion

The present work introduces an oblique pole-side test focused on the child's interactions with the vehicle interior to determine the body regions of interest and the injury criteria suffered by the child during the test. The child was positioned in the right rear seat (far-side impact) and the left rear seat (nearside impact) to represent a typical scenario where the child was positioned without any guidelines established by Road Traffic Regulators. For this numerical test, a CRS is not used, and the six-year-old child is only restrained by a 3-point seatbelt to find possible injuries in regions such as Head, Neck, and Thorax.

The lateral test was proposed as a complementary test to check the sensibility of the modified HBM PIPER and evaluate if the FE model was not affected during the positioning process in the PIPER software tool (v.1.1.0). The data from case 1 show a slightly non-significant difference in terms of the peak values reached and the path of the curves obtained in the shoulder and pelvis regions.

The FE FORD Explorer 2003 for the oblique pole-side impact was evaluated against the Explorer vehicle used for the crash tests 4471, 4563, and 4564 [32–34]. The FE FORD Explorer has an increment of 0.7 % on the ATW due to the numerical model incorporating the weight of the child. The acceleration data from the accelerometers of the FE model was correlated with the data from the laboratory test procedures according to ISO/TS 18571 [43]. The correlation of the signals was located at R3, which is a fair grade. Fig. 18 shows the acceleration responses from the FE model with the basic reference of the v4564 signal for y acceleration at the rear

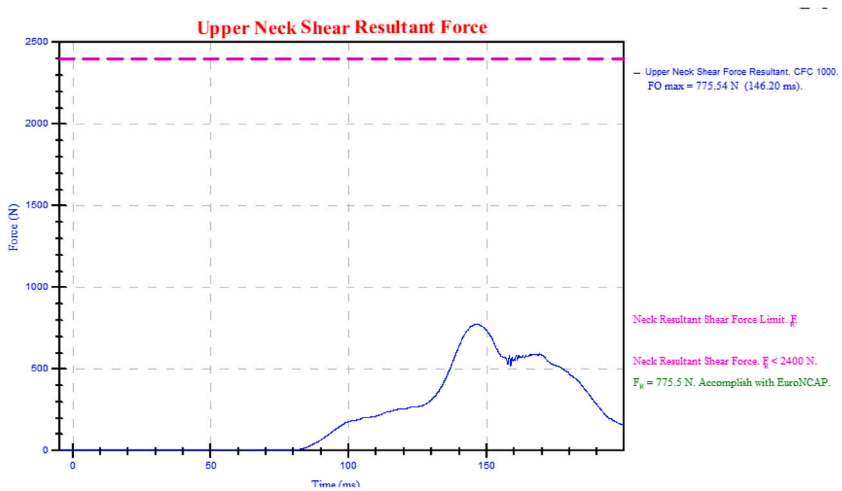

(a)

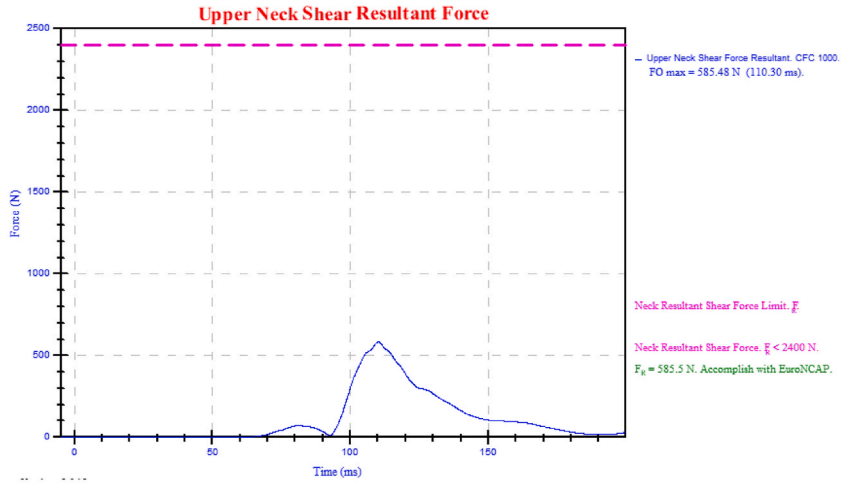

(b)

Fig. 15. Resultant force at the upper neck (a) far-side (b) nearside.

right seat. The model was tested with the original boundary conditions from the baseline FE Explorer model, but the correlation from the signals was worse, so new contact formulations between the interior components were applied to reach the actual accelerations data (defined by materials and methods) this behavior was not found in the numerical frontal test that were performed before by the IPN Biomechanics Applied Laboratory [44,45].

The results obtained by the Piper Child model in the oblique pole-side impact showed some factors that have the potential to affect the injury outcomes suffered by the child. These factors were the child-door interaction, the seatbelt, the child's posture, the child's anthropometric dimensions, and the lack of a CRS. Additionally, it was observed that if the lap and shoulder belts did not fit properly, the shoulder belt slipped off the shoulder, exerting pressure on the neck, increasing the head excursion and a higher injury risk into the Head, Thorax, and Neck. The findings suggests that the values obtained indicate that the sliding behavior observed needs a more detailed study to define better contact interacción between the child and the seat, also an improcedente of the geometric and material properties of the seat. Therefore, additional numerical and experimental tests should be carried out to establish the influence exerted by the parameters set out before. The Side Impact Criteria selected to compare the injuries obtained in the nearside and far-side impact configuration were according to the EURO NCAP because other traffic regulators do not have well-defined injury criteria for side impact where the limits for the different body regions of a child are defined. Also, the criteria were considered with limitations because these criteria are not defined for an oblique pole-side impact. The NCAP protocol for the Side Impact Mobile Deformable Barrier testing protocol defined the criteria.

The study has some limitations. First, the FE Ford Explorer was adjusted to the ATW. Still, the exact distribution of vehicle weight as the databases for the frontal and rear zone cannot be replicated precisely. The measurements have differences from the experimental

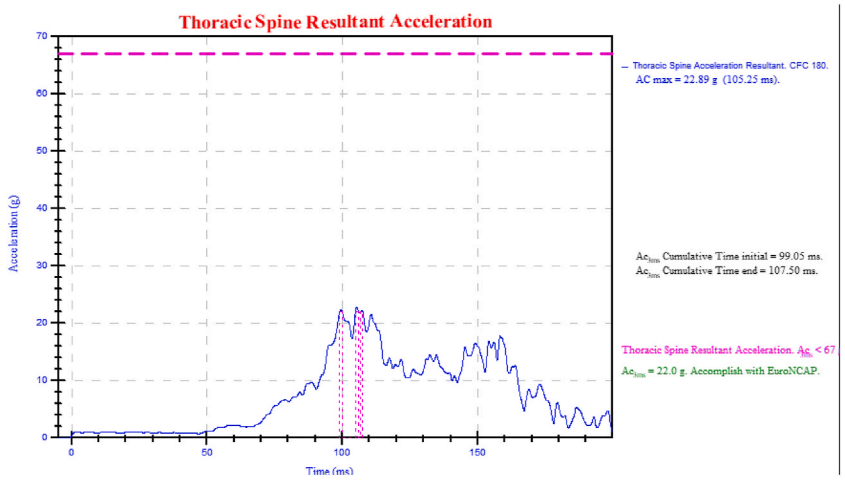

(a)

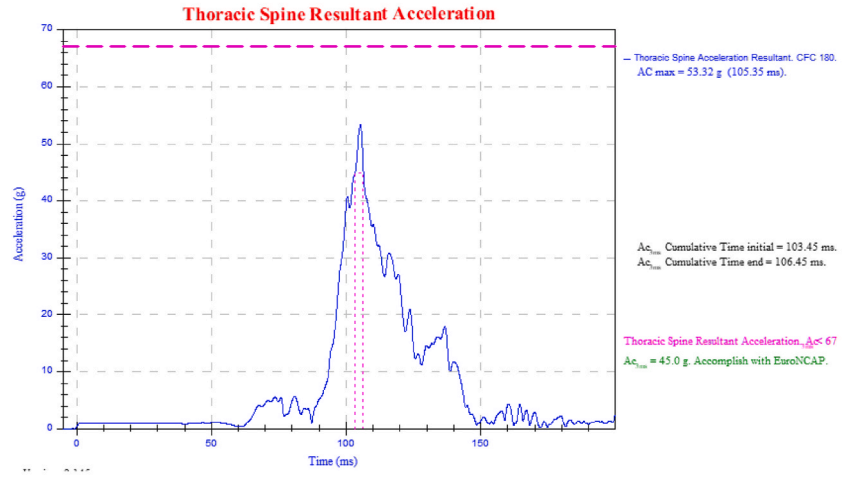

(b)

Fig. 16. Thoracic spine resultant acceleration by the PIPER child a) far-side b) nearside.

model for several reasons, such as the FE Explorer does not have the same number of components, the thickness for the components differs from the fabricated model, the materials properties, and the numerical model does not have the same welding points. The formulations for the contacts between the components affect the data collected from the model, producing higher variations in the correlation between the laboratory signal and the numerical. Additional tests need to be performed to investigate the influence of the previous factor on the Explorer measurements in a lateral test. Another limitation is that the PIPER child model neck has an excessive neck rotation during the oblique pole-side test, so an additional test is proposed to check if the neck's materials occasioned the behavior or if contact with the seatbelt produced it. The study can be extended in the future with more numerical or experimental tests with different vehicles, the use of other Child HBMs and child ATDs, and the incorporation of the different CRSs available in the market.

5. Conclusion

The data obtained in this work provides a first perspective on the importance of conducting oblique pole-side impact studies to understand children's behavior in this crash configuration and the importance of emphasizing the use of Child Restraint Systems in countries where CRS are not considered for child security.

The evaluations proposed demonstrate that a positioning process with the correct postprocessing has no impact on the skin mesh, the body geometry, and contacts from the interior of the body model. The slight differences at peak values or the path signal can be correlated to the change of position of the impact and the contact area between the model and the impactor.

The results obtained through the oblique pole-side test show that the HBM omnidirectional property has the potential to provide

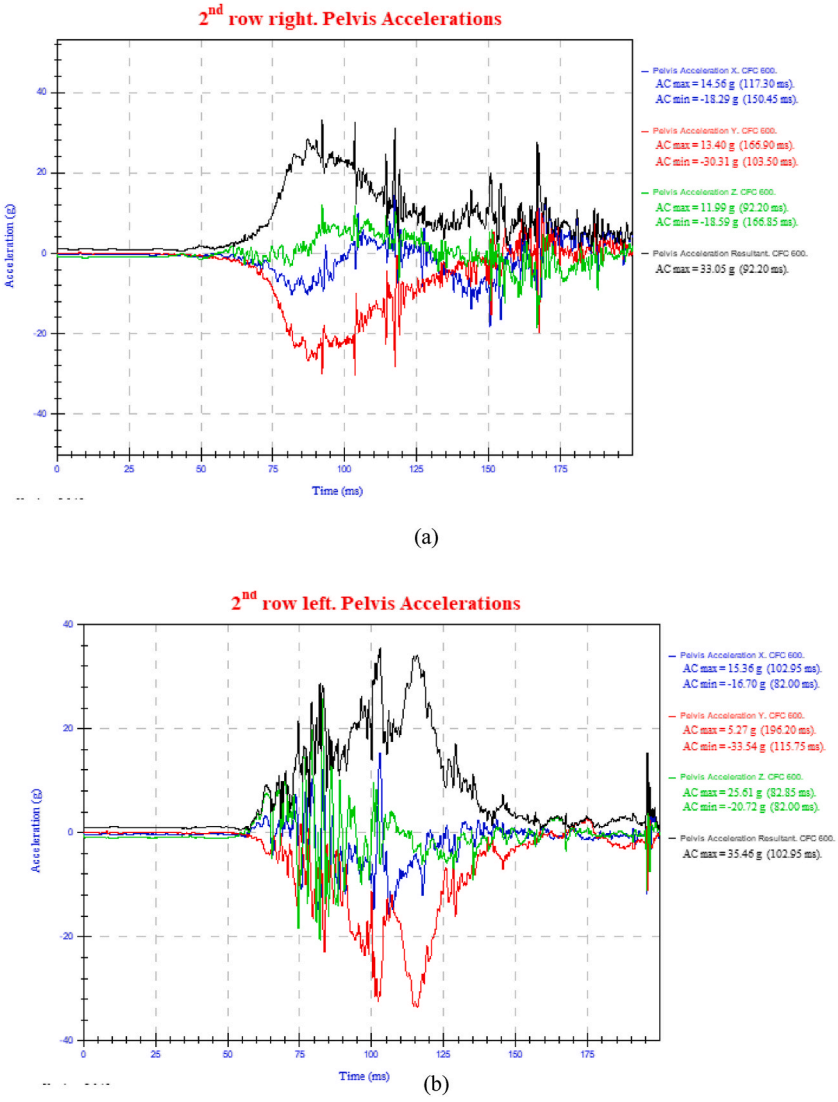

Fig. 17. Pelvis acceleration by the 6yo PIPER a) far-side b) nearside.

significant data on child responses to different child road traffic injuries. However, some revisions need to be made to the vehicle and child model. The Explorer model needs to consider more vehicle interior components, such as door trims, detailed rear seats, and a revision between the contacts defined to the vehicle components. In contrast, the PIPER child model needs an evaluation of interior body parts such as the Head and Pelvis regions because they are the body regions with more noise for the data collected.

For both oblique pole-side impacts, the HBM PIPER interaction with the rear seat demonstrates that the submarine effect needs to be addressed by posterior researchers.

Data availability statement

The authors do not have permission to share data.

Funding

The authors are thankful to the Consejo Nacional de Humanidades, Ciencia y Tecnología (CONAHCyT), the Instituto Politécnico Nacional for the support received in SIP 20240701 and SIP 20242785, EDI grant, all from SIP/IPN and The Ministerio de Ciencia, Innovación y Universidades and Fondo Europeo de Desarrollo Regional (FEDER) for the project ELAST with reference: PID2021-123978NB-I00.

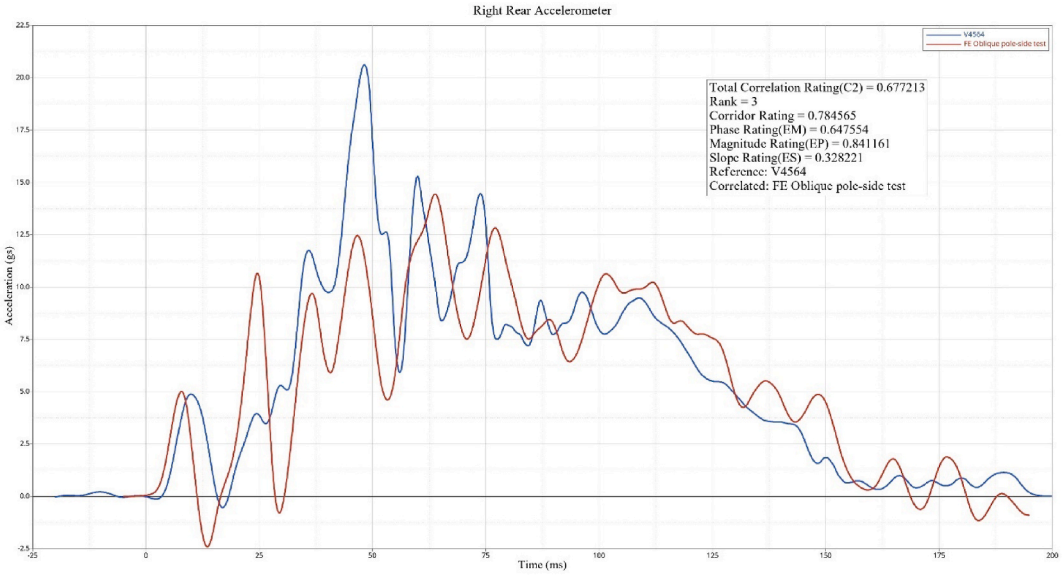

Fig. 18. ISO 18571 correlation for the y-acceleration pulse collected for the right rear accelerometer.

CRediT authorship contribution statement

Jose L. Torres-Ariza: Writing – review & editing, Writing – original draft, Methodology, Investigation, Formal analysis, Conceptualization. **Luis Martínez Sáez:** Writing – review & editing, Writing – original draft, Supervision, Project administration. **Christopher R. Torres-San Miguel:** Writing – review & editing, Writing – original draft, Supervision, Conceptualization.

Declaration of competing interest

The authors declare that they have no known competing financial interests or personal relationships that could have appeared to influence the work reported in this paper.

Appendix A. Supplementary data

Supplementary data to this article can be found online at https://doi.org/10.1016/j.heliyon.2024.e35927.

References

[1] INSP, México, séptimo lugar mundial en siniestros viales. https://www.insp.mx/avisos/4761-seguridad-vial-accidentes-transito.html, 2020.
[2] World Health Organization, Road traffic injuries, (222AD). https://www.who.int/news-room/fact-sheets/detail/road-traffic-injuries.
[3] UNICEF, A League Table of Child Deaths by Injury in Rich Nations, UNICEF Innocenti Research Centre, Florence, 2001.
[4] United Nations, Honour traffic victims by making roads safer: Guterres, UN News (2022). https://news.un.org/en/story/2022/11/1130892.
[5] EURO NCAP, Side Mobile Barrier, (n.d.). https://www.euroncap.com/en/car-safety/the-ratings-explained/adult-occupant-protection/lateral-impact/side-mobile-barrier/.
[6] G.R. Whitman, D'Aurelio Louis, B.J. Benda, L. Sicher, A. V. Hart, Considerations for Optimizing Occupant Protection to Children in Side Impact Crashes, Pennsylvania, n.d.
[7] F.A. Pintar, D.J. Maiman, N. Yoganandan, Injury patterns in side pole crashes, Annu. Proc. Assoc. Adv. Automot. Med. 51 (2007) 419–433.
[8] K. Weber, Crash Protection for Child Passengers: A Review of Best Practice, 2000.
[9] L.K. Sullivan, A.E. Louden, NHTSA'S initial evaluation of Child Side Impact test procedures, in: 21st International Technical Conference on the Enhance Safety of Vehicles, NHTSA, Stuttgart, 2009.
[10] K.B. Arbogast, E.K. Moll, S.D. Morris, R.L. Anderko, D.R. Durbin, F.K. Winston, Factors influencing pediatric injury in side impact collisions, Annu. Proc. Assoc. Adv. Automot. Med. 44 (2000) 407–428.
[11] National Highway Traffic Safety Administration, FMVSS No 214, Dynamic Side Impact Protection, Rigid Pole Side Impact Test Requirements, 2012. Washington.
[12] European New Car Assessment Programme, Oblique Pole Side Impact Testing Protocol, 2021.
[13] UNECE, Global Technical Regulation No.14 (Pole Side Impact) ECE/TRANS/180/Add, vol. 14, 2014.
[14] National Center for Statistics and Analysis, FMVSS No. 214: Amending Side Impact Dynamic Test Adding Oblique Pole Test, 2007.
[15] M. Selvamanikandan, S. Venkatesan, Improvements of side oblique Pole impact safety performance using finite element method, Int. J. Eng. Res. V9 (2020), https://doi.org/10.17577/IJERTV9IS030530.
[16] E. Lee, A. Shrivatri, S. Ohara, NHTSA oblique test data analysis method by LS-DYNA modeling, in: 25th International Technical Conference on the Enhanced Safety of Vehicles (ESV), NHTSA, Detroit, 2017.

[17] L. Pengtao, Y. Jiong, Z. Xiying, Modeling and simulation analysis of pole side impact crash test sled, International Journal of Research in Engineering and Science (IJRES) 3 (2015) 1–4.
[18] P. Beillas, X. Wang, B. Frechede, T. Janak, PIPER Final Publishable Summary, 2017.
[19] P. Beillas, A. Le Ruyet, M.-C. Chevalier, Side impact applications of the PIPER scalable child human body model, in: 15th International Conference Protection of Children in Cars, 2017.
[20] M. Fahlstedt, S. Kleiven, X. Li, The Influence of the Body on Head Kinematics in Playground Falls for Different Age Groups, International Research Council on the Biomechanics of Injury, IRCOBI, Athens, 2018, pp. 336–337.
[21] M. Miller, D. Perez-Rapela, B. Gepner, M. Edwards, J. Jermakian, A Methodology for LArge-Scale Parametric Evaluation of Child Booster Seats, International Research Council on the Biomechanics of Injury, 2021, pp. 593–615. IRCOBI 2021.
[22] J. Maheshwari, A. Belwadi, A pilot study evaluating the 3-point and 4-point restraint system for pediatric occupants in nonstandard seating positions, Traffic Inj. Prev. 20 (2019) S203–S204, https://doi.org/10.1080/15389588.2019.1665430.
[23] J. Holtz, Comparison of PIPER Child Human Body Model and Q6 Dummy Analysing Sensors of the HBM, International Research Council on the Biomechanics of Injury, 2019, pp. 127–128. IRCOBI.
[24] J. Maheshwari, N. Duong, S. Sarfare, A. Belwadi, Evaluating the response of the PIPER scalable human body model across child restraining seats in simulated frontal crashes, Traffic Inj. Prev. 19 (2018) S140–S142, https://doi.org/10.1080/15389588.2018.1532204.
[25] C. Giordano, S. Kleiven, Development of a 3-Year-Old Child FE Head Model, Continuously Scalable from 1.5-to 6-Year-Old, International Research Council on the Biomechanics of Injury, IRCOBI, 2016, pp. 288–302.
[26] J. Maheshwari, S. Sarfare, C. Falciani, A. Belwadi, Pediatric occupant human body model kinematic and kinetic response variation to changes in seating posture in simulated frontal impacts – with and without automatic emergency braking, Traffic Inj. Prev. 21 (2020) S49–S53, https://doi.org/10.1080/15389588.2020.1825699.
[27] A. Belwadi, S. Sarfare, S. Tushak, J. Maheshwari, S. Menon, Responses of the scaled pediatric human body model in the rear- and forward-facing child seats in simulated frontal motor vehicle crashes, Traffic Inj. Prev. 20 (2019) S143–S144, https://doi.org/10.1080/15389588.2019.1661684.
[28] C. Giordano, X. Li, S. Kleiven, Performances of the PIPER scalable child human body model in accident reconstruction, PLoS One 12 (2017) e0187916, https://doi.org/10.1371/journal.pone.0187916.
[29] J. Berntsson, A Parametric Study of Shoulder Belt Interactions with the PIPER Scalable Child Human Body Model in Frontal and Frontal Offset Impacts, Master's Thesis, Chalmers University of Technology, 2018. https://odr.chalmers.se/items/92f5c361-48d9-476b-aafa-eb001652f708.
[30] M. Daouacher, Evaluation of Occupant Kinematics in Crash Using the PIPER Model, Master Thesis, Karlstads University, 2019. http://kau.diva-portal.org/smash/record.jsf?pid=diva2%3A1340871&dswid=-4257.
[31] S.K. Jóhannsdóttir, Evaluation of Head and Neck Injuries during Misuses of Child Restraint Systems, Master Thesis, KTH Royal Institute of Technology School of Engineering Sciences in Chemistry, Biotechnology and Health, 2019.
[32] MGA Research Corporation, Full Scale Side Impact Pole Tests of Baseline Vehicles: Report Number TO11-MGA-2003-001, 2003. Burlington, Wisconsin.
[33] MGA Research Corporation, Full Scale Side Impact Pole Tests of a Baseline Vehicles: Report Number TO11-MGA-2003-006, 2003. Burlington Wisconsin.
[34] MGA Research Corporation, Full scale side impact Pole test of baseline vehicles: report number To11-MGA-2003-004. https://nrd-static.nhtsa.dot.gov/reports/vehdb/v00000/v04500/v04564R001.pdf, 2003.
[35] P. Baranowski, K. Damaziak, L. Mazurkiewicz, J. Malachowski, A. Muszynski, D. Vangi, Analysis of mechanics of side impact test defined in UN/ECE Regulation 129, Traffic Inj. Prev. 19 (2018) 256–263, https://doi.org/10.1080/15389588.2017.1378813.
[36] S. Kang, C. Chen, S. Guha, M. Paladugu, M. Sundaram Ramasamy, L. Gade, F. Zhu, LS-DYNA belted occupant model, in: 15th International LS-DYNA Users Conference, 2018. Detroit.
[37] National Highway Traffic Safety Administration, Crash Simulation Vehicle Models, (n.d.).
[38] P. Beillas, C. Giordano, V. Alvarez, X. Li, X. Ying, M.-C. Chevalier, S. Kirscht, S. Kleiven, Development and performance of the PIPER scalable child human body models, in: 14 Th International Conference Protection of Children in Cars, Munich, 2016.
[39] A.L. Irwin, H.J. Mertz, A.M. Elhagediab, S. Moss, Guidelines for assessing the biofidelity of side impact dummies of various sizes and ages. https://doi.org/10.4271/2002-22-0016, 2002.
[40] J. Ouyang, Q. Zhu, W. Zhao, Y. Xu, W. Chen, S. Zhong, Experimental cadaveric study of lateral impact of the pelvis in children, Di Yi Jun Yi Da Xue Xue Bao 23 (2003) 397–401, 408.
[41] SAE, Instrumentation for Impact Test Part 1 - Electronic Instrumentation J211/1_202208, 2022.
[42] Euro NCAP, Assessment Protocol - Child Occupant Protection Version 8.1, 2023.
[43] ISO/TS 18571:2024 Road Vehicles — Objective Rating Metric for Non-ambiguous Signals, 2024.
[44] I.L. Cruz-Jaramillo, C.R. Torres-SanMiguel, J.A. Leal-Naranjo, L. Martínez-Sáez, Numerical child restraint system analysis in 6 years old infant during a dolly rollover test, Int. J. Crashworthiness 26 (2021) 404–412, https://doi.org/10.1080/13588265.2020.1718464.
[45] I.L. Cruz-Jaramillo, C.R. Torres-San Miguel, L. Martínez-Sáez, V. Ramírez-Vela, G.M. Urriologoitia-Calderón, Numerical low-back booster analysis in a 6-year-old infant during a dolly rollover test, J. Adv. Transport. 2020 (2020) 1–9, https://doi.org/10.1155/2020/5803623.